Environmental Toxicology and Chemistry—Volume 39, Number 12—pp. 2496–2508, 2020
Received: 17 July 2020 | Revised: 18 August 2020 | Accepted: 8 September 2020

Environmental Toxicology

The Combined Algae Test for the Evaluation of Mixture Toxicity in Environmental Samples

Lisa Glauch[a] and Beate I. Escher[a,b,*]

[a]Helmholtz Centre for Environmental Research, Leipzig, Germany
[b]Center for Applied Geoscience, Eberhard Karls University of Tübingen, Tübingen, Germany

Abstract: The combined algae test is a 96-well plate-based algal toxicity assay with the green algae *Raphidocelis subcapitata* that combines inhibition of 24-h population growth rate with inhibition of photosynthesis detected after 2 and 24 h with pulse-amplitude modulated (PAM) fluorometry using a Maxi-Imaging PAM. The combined algae test has been in use for more than a decade but has had limitations due to incompatibilities of the measurements of the 2 biological endpoints on the same microtiter plates. These limitations could be overcome by increasing growth rates and doubling times on black, clear-bottom 96-well plates by application of dichromatic red/blue light-emitting diode illumination. Different robotic dosing approaches and additional data evaluation methods helped to further expand the applicability domain of the assay. The combined algae test differentiates between nonspecifically acting compounds and photosynthesis inhibitors, such as photosystem II (PSII) herbicides. The PSII herbicides acted immediately on photosynthesis and showed growth rate inhibition at higher concentrations. If growth was a similar or more sensitive endpoint than photosynthesis inhibition, this was an indication that the tested chemical acted nonspecifically or that a mixture or a water sample was dominated by chemicals other than PSII herbicides acting on algal growth. We fingerprinted the effects of 45 chemicals on photosynthesis inhibition and growth rate and related the effects of the single compounds to designed mixtures of these chemicals detected in water samples and to the effects directly measured in water samples. Most of the observed effects in the water samples could be explained by known photosystem II inhibitors such as triazines and phenylurea herbicides. The improved setup of the combined algae test gave results consistent with those of the previous method but has lower costs, higher throughput, and higher precision. *Environ Toxicol Chem* 2020;39:2496–2508. © 2020 The Authors. *Environmental Toxicology and Chemistry* published by Wiley Periodicals LLC on behalf of SETAC.

Keywords: Algae; Aquatic toxicology; Effects-based monitoring; Herbicide; Mixture toxicology; Photosynthesis inhibition

INTRODUCTION

The combined algae test (Escher et al. 2008) has been in use for more than a decade in water quality monitoring (Escher et al. 2009; Vermeirssen et al. 2010; Margot et al. 2013; Tang et al. 2013; Di Paolo et al. 2016; Neale et al. 2017; Kienle et al. 2019) and for investigation of transformation processes (Mestankova et al. 2011). It is a 96-well-plate–based assay that combines the quantification of photosynthesis inhibition with inhibition of growth rate and can differentiate between such herbicides that directly act on photosystem II (PSII) and chemicals and herbicides with other modes of action. Thus, it combines diagnostic features with quantification of algal toxicity.

At the time of its development prior to 2008, illumination technology had not been at a developmental stage to achieve satisfactory growth of algae in black clear-bottom multiwell plates, but these limitations were then overcome by a custom-built well-plate illuminator that used red and blue light-emitting diodes (LEDs) for optimum growth.

According to Organisation for Economic Co-operation and Development (OECD) test guideline 201 (2006), which requires that the assay be performed in glass flasks, the exponential algal growth rate should be 0.92 d^{-1}, which corresponds to a doubling time of 18 h. The corresponding International Organization for Standardization (ISO) method 8692 (2012) demands a doubling time of 12 h. To achieve exponential growth over 72 h in a growth inhibition assay, the experiment is started with only 10^4 cells/mL (Organisation for Economic

This article includes online-only Supplemental Data.

* Address correspondence to beate.escher@ufz.de
Published online 14 September 2020 in Wiley Online Library (wileyonlinelibrary.com).
DOI: 10.1002/etc.4873

Co-operation and Development 2006). This cell density is, however, too low to measure the inhibition of photosynthesis with the Maxi-Imaging pulse-amplitude modulated (PAM) device (Schreiber et al. 2007), which requires at least 10^6 cells/mL to ensure that inhibition of quantum yield of photosynthesis can already be detected after 2 h of exposure with the toxicant or sample. Therefore, the combined algae test (Escher et al. 2008) was developed as a compromise between inhibition of photosynthesis detected after 2- and 24-h growth rate inhibition and was started with 2×10^6 cells/mL if the green algae species *Racidophelis subcapitata* (previously called *Pseudokirchneriella subcapitata*) was used. Other studies that focused exclusively on PAM measurements used 10^7 cells/mL (de Baat et al. 2018), which would not be compatible with growth assays.

The exposure duration of the combined algae test is limited to 24 h. Chemicals of a wide range of hydrophobicity, including ionic organic chemicals, were shown to obtain steady state within minutes to hours in green algae (Vogs et al. 2015). Consequently, if growth rate remains exponential during the entire incubation time and the chemical does not degrade, there should not be a large difference in the sensitivity between 24 and 72 h for baseline toxicity.

Growth rates were quantified via optical density measurements at 685 nm (Escher et al. 2008), which is not an optimal parameter because it is prone to artifacts when environmental samples are tested. Therefore, several studies have recommended quantification of growth rate with fluorescence (Eisentraeger et al. 2003; Fai et al. 2007). However, transparent plates had to be used to achieve any growth at all in 96-well plates under standard white-light illumination, which could not be combined with fluorescence due to light scattering (Eisentraeger et al. 2003). Black plates were shown to be better suited for PAM fluorometry (Schreiber et al. 2007).

The goal of the present study was to further refine the combined algae test and make it amenable to robotic high-throughput testing. Our main hypothesis was that by optimization of the growth rate on the microtiter plate we would substantially improve the combined algae test. To demonstrate this, we developed a novel illumination system for microtiter plates, which allowed growth in black clear-bottom well plates. Efficient illumination with lower light intensity can be achieved by dichromatic LED illumination with red and blue LEDs (Wagner et al. 2016). To further improve high-throughput testing, we combined the new setup with diverse dosing approaches and concentration–response assessments at low effect levels to permit analysis of samples with low pollution. This was inspired by an automated high-throughput algal assay in accordance with ISO method 8629 (2012) developed by Eisentraeger et al. (2004).

The optimized experimental protocol was validated by comparing it with previous fingerprinting of PSII herbicides and other chemicals and by developing new baseline toxicity quantitative structure–activity relationships (QSARs). The applicability of the combined algae test was further demonstrated with a case study on the water quality of a small river, which was impacted by both agriculture and wastewater treatment plants. Testing of environmental samples was complemented by designed mixture experiments to test whether the algal toxicity was mainly driven by PSII herbicides or by the large load of other organic micropollutants.

MATERIALS AND METHODS

Algae and culture

Raphidocelis subcapitata was obtained from the algae culture collection at Göttingen University (strain number 61.81). The growth medium for the algae was Talaquil (Le Faucheur et al. 2005). The assay was conducted in Talaquil medium fortified with 1.2 mM $NaHCO_3$ or 3.5 mM $NaHCO_3$ or with the pH-stabilized OECD medium (Altenburger 2010). Detailed information on the experiments is given in the Supplemental Data, Section S1. The workflow of algae cultivation and cell numbers at each stage are depicted in the Supplemental Data, Figure S1.

Algae illumination

The cultures were illuminated with a custom-built light box (Supplemental Data, Figure S2) using panels of red and blue LEDs (50% red, 50% blue; Barthelme LEDlight flex 14 10 Plant Growing Light) from top and bottom with light intensity adjusted with an LED converter (Barthelme LED driver LHV60,W24, Chromoflex dimmer 4.0). More homogeneous illumination was achieved by 2 glass diffusor plates above and below the algae, as depicted in the Supplemental Data, Figure S2 and described in the Supplemental Data, Section S2. The light box sat on a shaker (KS 260 control; IKA) housed in an incubator (HettCube 400R; Hettich) set at 23 °C (Supplemental Data, Figure S2). The light intensity was measured with a Quantum/Radiometer/Photometer probe (LI-189; LI-COR) with the probe tip in the region of the light box where the assay plates were situated. Light intensity was optimized by evaluating the homogeneity of the growth rate over the entire 96-well plate, selecting a light intensity that led to the highest growth rates (Supplemental Data, Figure S3). The final light intensity was adjusted to $100 \pm 10\,\mu mol\,s^{-1}\,m^{-2}$ and regularly checked and adjusted.

Optimization of growth

Cells were counted with a CASY counter (CASY TTT; OLS). The exponential growth rate constant μ was quantified by plotting the natural logarithm of the cell count CC normalized to the cell count at time 0 ($t0$) against the time and deriving μ by linear regression (Equation 1).

$$\ln\left(\frac{CC(t)}{CC(t0)}\right) = \mu t \quad (1)$$

Initially, we measured CC frequently to ensure exponential growth over the time of the experiment in the 96-well plates, but during toxicity testing of samples, we measured at 2 and

24 h and derived μ with Equation 2. The 2-h delay in the CC measurement ensured that the cells had returned to the exponential growth rate after the disturbance due to plating and dosing.

$$\mu = \frac{\ln\left(\frac{CC(t24)}{CC(t2)}\right)}{22\ h} \quad (2)$$

The doubling time t_{2x} was calculated with Equation 3.

$$t_{2x} = \frac{\ln(2)}{\mu} \quad (3)$$

Optical density at 685 nm (OD685) and fluorescence with excitation at 440 nm and emission at 685 nm (F440/685) were used as proxies for cell count.

Combined algae test

The workflow of the combined algae test is outlined in Figure 1, with details given in the Supplemental Data, Figure S4. Algae were cultured as described in the Supplemental Data, Section S1. Dosing plates (96-well black clear-bottom plates (Corning CLS 3603) were prepared according to the plate design in Supplemental Data, Figure S5 with 7 samples and diuron as quality control in 10-step dilution series. Water extracts and chemicals were solvent-exchanged into medium by blowing down methanol or other solvents used and redissolving the residue in medium. For water extracts, the pH was checked, and if required, adjusted to pH 7 with 5 M NaOH. Serial dilutions were pipetted manually with an electronic multichannel pipette (Xplorer 50-1200 μL; Eppendorf). Linear dilutions were prepared with a pipetting robot (Hamilton Microlab Star) according to Escher et al. (2019). Neat liquid compounds and dimethyl sulfoxide (DMSO) stocks were printed into the dosing plates using a Tecan D300e Digital Dispenser as described previously (Escher et al. 2019).

The dosing plates were mixed with a BioShake iQ (QInstruments) at 1000 rpm for 30 s, and OD685 and F440/685 were read with a plate reader (Tecan Infinite M200 Pro). For F440/685, the measurement was taken from the top with a manual Z-position of 20 mm. The sample was excited with 440 nm, and emission was read at 685 nm with 25 flashes, gain 100, and 20-μs integration time.

Then 150 μL of the algae suspension freshly resuspended in medium at 4×10^6 cells/mL was added to each well of the 96-well plate (now termed the assay plate; Supplemental Data, Figure S4).

Water evaporation poses a problem during plate-based assays if original covers are used (Eisentraeger et al. 2004) and sealing with Parafilm might lead to water condensation at the cover; thus contamination of neighboring wells is possible. We used adhesive gas-permeable plate covers (Moisture Barrier Seal 96; 4titude), shook the plates at 1600 rpm, and centrifuged at 100 *g* for 1 min (Megafuge 40; Thermo Scientific) prior to measurements at 2 and 24 h to bring condensed water back to the well. We removed the sealing before each

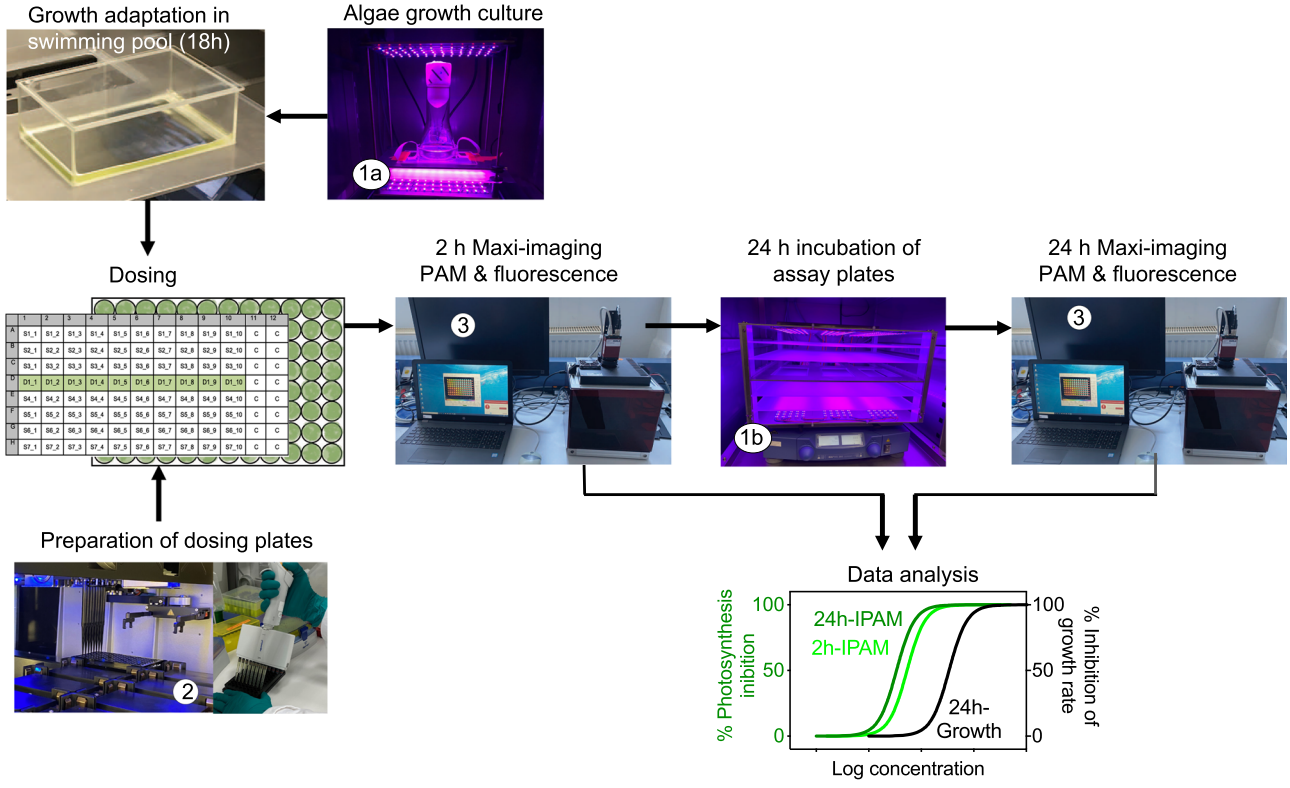

FIGURE 1: Workflow of the combined algae test. The instruments used are 2 custom-built light boxes, which are on a shaking platform in an incubator (1a and 1b), a pipetting robot (2), the Maxi-Imaging pulse-amplitude modulated (PAM) device (3), and a plate reader (not shown). Details of the algae culture are given in Supplemental Data, Figure S1, on the illumination in Supplemental Data, Figure S2, on the assay workflow in Supplemental Data, Figure S4, and on the details of the dosing plate design in Supplemental Data, Figure S5.

measurement. Afterward the plate was covered up with a new gas-permeable seal.

As described in the Supplemental Data, Figure S4, OD685 and F440/685 were read immediately and after 2 and 24 h of exposure. The yield Y of photosynthesis in PSII (Supplemental Data, Equation S1) was measured with a Maxi-Imaging PAM fluorometer (IPAM; Walz) after 2-h exposure and after 24-h exposure according to (Escher et al. 2008) with the settings given in the Supplemental Data, Figure S6. The percentage of inhibition of photosynthesis was calculated with Equation 4, where Y_{sample} is Y of the chemical or sample tested and $Y_{control}$ is the average Y of the unexposed algae (average of 16/96 wells; see plate layout in the Supplemental Data, Figure S5.

$$\%\ \text{inhibition of photosynthesis} = 1 - \frac{Y_{sample}}{Y_{control}} \quad (4)$$

The fluorescence was measured before and directly after the addition of the algae as well as after 2 and 24 h of exposure in the light box, shaken at 90 rpm at 23 °C.

In analogy, the inhibition of growth rate was calculated from the 24-h growth rate μ of the sample μ_{sample} and the control $\mu_{control}$ (Equation 5). The growth rate was log-linearly interpolated from the measurement of fluorescence F440/685 at 2 and 24 h (Equation 2).

$$\%\ \text{inhibition of growth rate} = 1 - \frac{\mu_{sample}}{\mu_{control}} \quad (5)$$

If a chemical or sample tested had autofluorescence, a blank read of the $\text{fluorescence}_{440/685}$ in the well should be added and subtracted from the fluorescence signal of chlorophyll (Equation 6) prior to adding the cells.

$$\mu = \frac{\ln\left(\frac{F440/685(t24) - F440/685(\text{sample autofluorescence})}{F440/685(t2) - F440/685(\text{sample autofluorescence})}\right)}{22\ \text{h}} \quad (6)$$

The biomass endpoint was assessed either via the cell count (here quantified with a CASY counter; Equation 7) or via the optical density at 685 nm (OD685; Equation 8).

$$\%\ \text{inhibition of cell count} = 1 - \frac{CC_{sample}}{CC_{control}} \quad (7)$$

$$\%\ \text{inhibition of biomass} = 1 - \frac{OD685_{sample} - OD685_{sample\ blank}}{OD685_{control} - OD685_{sample\ blank}} \quad (8)$$

We used the biomass endpoints for method optimization but in routine testing of chemicals and samples the growth rate measured via fluorescence was used.

Data evaluation

The concentration–response curves of all 3 endpoints were fitted to a log–logistic function (Equation 9) with a fixed minimum at a 0% effect and a fixed maximum at a 100% effect. Adjustable parameters were the slope and the concentrations causing a 50% effect (EC50).

$$\%\ \text{inhibition} = \frac{100\%}{1 + 10^{\text{slope} \times (\log EC50 - \log \text{concentration})}} \quad (9)$$

The endpoint used for reporting was the EC10, the concentration causing 10% of the maximum effect, which can be calculated directly by transforming the concentration–response curve with Equation 10.

$$\log EC10 = \log EC50 + \frac{1}{\text{slope}} \log\left(\frac{100\% - 10\%}{10\%}\right) \quad (10)$$

At effect levels <30% the log–logistic curves become close to linear on a linear concentration scale (Escher et al. 2018a). Thus, Equation 11 can be applied.

$$\text{effect } y = \text{slope} \times \text{concentration} \quad (11)$$

The EC10 can be derived from the linear concentration–response curve with Equation 12 with the standard error SE (EC10) given by Equation 13.

$$EC10 = \frac{10\%}{\text{slope}} \quad (12)$$

$$SE(EC10) = \frac{10\%}{\text{slope}^2} \times SE(\text{slope}) \quad (13)$$

Baseline toxicity QSARs

A test set of 7 baseline toxicants (2-allylphenol, 2-butoxyethanol, 4-chloro-3-methylphenol, 3-nitroaniline, 4-pentylphenol, 2-phenylphenol, and 2,4,5-trichloroaniline) that had been used previously to set up baseline toxicity QSARs (Vaes et al. 1998) was tested again to confirm the validity of the previously established baseline toxicity QSAR for the combined algae test (Escher et al. 2008; Tang and Escher 2014).

Test chemicals

Fourty-four chemicals were tested, among them 20 PSII herbicides (ametryn, atrazine, bentazon, bromacil, chloridazon, diuron, fenuron, fluometuron, hexazinone, isoproturon, lenacil, metamitron, metribuzin, prometryn, propanil, propazine, simazine, simetryn, terbuthylazine, terbutryn), 11 transformation products of PSII herbicides (atrazine-2-hydroxy, atrazine-desethyl, atrazine-desisopropyl, chloridazon-desphenyl, chloridazon-methyldesphenyl, diuron-desdimethyl [3,4-dichlorophenylurea], metamitron-desamino, simazine 2-hydroxy, terbuthylazine-desethyl, terbuthylazine-2-hydroxy, and terbuthylazine-desethyl-2-hydroxy), and 13 other environmentally relevant chemicals and herbicides with other modes of action that had been detected in surface waters (1H-benzotriazole, 4-aminoantipyrine [ampyrone], benzothiazole-2-sulfonic acid, carbamazepine, denatonium, diclofenac, ketamine, 2-methyl-4-chlorophenoxyacetic acid (MCPA), mecoprop, N-acetyl-4-aminoantipyrine [4-acetaminoantipyrine], N-formyl-4-aminoantipyrine, tebuconazole, and triclosan). In

addition, the solvents methanol and DMSO were tested. All chemicals, their DSSTox substance identifier (DTXSID), octanol/water partition constant K_{OW}, acidity constant, and speciation and liposome water distribution ratio at pH 7.4 log D_{lipw} (pH 7.4) are listed in the Supplemental Data, Table S2.

Water samples

The surface water samples had been collected at the Ammer River (Germany) and tested in various other bioassays in a previous study (Müller et al. 2018). In total, 529 organic chemicals were analyzed with liquid chromatography–mass spectrometry as described by Neale et al. (2020). The wastewater treatment influent and effluent samples were taken from the inlet and outlet of an horizontal intensified treatment wetland described in more detail by Nivala et al. (2018), but samples were taken anew for demonstration purpose.

Iceberg modeling

The diuron equivalent concentrations (DEQ_{bio}) for the 3 endpoints of inhibition of photosynthesis after 2-h exposure (2-h IPAM-DEQ_{bio}), inhibition of photosynthesis after 24-h exposure (24-h IPAM-DEQ_{bio}), and inhibition of growth (24-h Growth-DEQ_{bio}) were calculated from the $EC10_{diuron}$ of the reference compound diuron and the $EC10_{sample}$ of the sample for each endpoint (Equation 14, SE in Equation 15). Because the units of the $EC10_{sample}$ are in relative enrichment factors, the final unit of DEQ_{bio} is ng_{diuron}/L.

$$DEQ_{bio} = \frac{EC10_{diuron}}{EC10_{sample}} = \frac{slope_{sample}}{slope_{diuron}} \quad (14)$$

$$SE(DEQ_{bio}) \approx \sqrt{\frac{1}{EC10_{sample}^2} \times SE(EC10_{diuron})^2 + \frac{EC10_{diuron}^2}{EC10_{sample}^4} \times SE(EC10_{sample})^2} \quad (15)$$

The diuron equivalent concentrations DEQ_{chem} (Equation 16 and SE in Equation 17) can also be predicted from the detected concentrations C_i of all chemicals i and their relative effect potency (REP_i; Equation 18).

$$DEQ_{chem} = \sum_{i=1}^{n} REP_i \times C_i \quad (16)$$

$$SE(DEQ_{chem}) \approx \sqrt{\sum_{i=1}^{n} C_i^2 \times SE(REP_i)^2 + REP_i^2 \times SE(C_i)^2} \quad (17)$$

$$REP_i = \frac{EC10_{diuron}}{EC10_i} = \frac{slope_i}{slope_{diuron}} \quad (18)$$

Mixture experiments

Mixture experiments were performed with 10 PSII herbicides or their transformation products (ametryn, atrazine, atrazine-desethyl, diuron, isoproturon, lenacil, metribuzin, terbuthylazine, terbuthylazine-desethyl, and terbutryn) and 10 other chemicals (1H-benzotriazole, benzothiazole-2-sulfonic acid, denatonium, diclofenac, ketamine, MCPA, mecoprop, N-formyl-4-aminoantipyrine, tebuconazole, and triclosan) in 3 groups: A) 10 PSII herbicides, B) 10 other chemicals, and C) all 20.

First, equipotent mixture ratios were prepared according to the ratios of $EC10_{2h\ IPAM}$ and $EC10_{24h\ IPAM}$. Note that the mixture ratios were not precise because they were designed using a preliminary EC10, and the final EC10 values for the single chemicals were obtained in parallel with the mixture experiments. The mixture predictions were made with the final EC10 data using the concentration ratios that were tested.

The mixture EC10 for linear concentration–response curves can be predicted for concentration addition and independent action with a simplified joint concentration/addition model (Equation 19) applicable only at low effect levels (<30%) for a mixture composed of n components i, present in fractions p_i, with $p_i = \frac{C_i}{C_{tot}}$ and $\sum p_i = 1$ (Escher et al. 2020b).

$$EC10(mixture) = \frac{1}{\sum_{i=1}^{n} \frac{P_i}{EC10}} = \frac{1}{\sum_{i=1}^{n} \frac{p_i \times slope_i}{10\%}} = \frac{10\%}{\sum_{i=1}^{n} p_i \times slope_i} \quad (19)$$

RESULTS AND DISCUSSION

Growth in the "swimming pool"

In the workflow of the combined algae test, the algae were taken from the sterile culture in the Erlenmeyer to the microplate assay format via an intermediate step in a glass reservoir in the shape of a microtiter plate, henceforth called the "swimming pool" (see photo at top left in Figure 1), where the algae were acclimatized to the format of the assay (for more details, see Supplemental Data, Section S2). The doubling time t_{2x} in the swimming pool was 15.5 ± 4.0 h ($n = 13$, coefficient of variation [CV] = 26%) at $100 \pm 10\ \mu mol\ s^{-1}\ m^{-2}$, thereby meeting the requirements of OECD test guideline 201 of t_{2x} 18 h (Organisation for Economic Co-operation and Development 2006) and almost the t_{2x} of 12 h of ISO method 8692 (International Organization for Standardization 2012).

Growth on black clear-bottom 96-well plate

Growth rates of algae on the plate could not routinely be quantified with the CASY counter as was done for the swimming pool. In the original version of the combined algae test (Escher et al. 2008), optical density was used as a proxy for cell counts but with the change from clear plates to black clear-bottom plates, fluorometric quantification can be used, which had been recommended for algal growth assays (Eisentraeger et al. 2003). The calibration of cell count versus the OD685 and fluorescence F440/685 is described in detail in the Supplemental Data, Section S4 and Figure S7, including a discussion on the impact of PSII inhibitors on F440/685.

The growth was exponential until 32 h, extending beyond the exposure duration of the combined algae test (Supplemental Data, Figure S8A). The growth rate and t_{2x}

depended on the starting algal density (Supplemental Data, Figure S8B). Growth was best with a low starting cell count of $<10^6$ cells/mL (t_{2x} of 12–14 h over 30 h), but this is not sufficient for the Multi-Imaging PAM measurements, so the starting algal density chosen was 2×10^6 cells/mL (t_{2x} of 14–15 h over 32 h), as in the original version of the combined algae test.

The doubling time t_{2x} on clear 96-well plates at illumination with $100 \pm 10\,\mu mol\,s^{-1}\,m^{-2}$ measured via optical density OD685 was 21.9 ± 2.0 h, which was indistinguishable from the t_{2x} of 22.8 ± 2.0 h on black clear-bottom plates in the same experiment. The stability of the growth rate and associated doubling times was high over repeated 24-h exposure experiments: t_{2x} was 22.3 ± 5.3 (24% CV, $n = 17$) when measured with the CASY, and t_{2x} was 22.9 ± 2.7 (12% CV, $n = 27$) when measured with optical density. This t_{2x} is higher than the requirements of OECD test guideline 201 (Organisation for Economic Co-operation and Development 2006) and ISO method 8692 (International Organization for Standardization 2012) but as good as the t_{2x} of 21 h with white light illumination in an INFORS incubator at $267\,\mu mol\,s^{-1}\,m^{-2}$ using Talaquil medium supplemented with 3.5 mM $NaHCO_3$ (Escher 2008). Also note that the dedicated growth experiments that went over 32 h (Supplemental Data, Figure S8) gave lower doubling times than the routine 24-h experiments, presumably because of a slight delay in onset of the growth after plating.

The custom-built light box with blue/red LED can not only be assembled at very low cost but it has also very low energy requirements and can possibly be further tuned to improve growth by mixing different ratios of blue and red LEDs. Wagner et al. (2016) demonstrated on the example of *Chlamydomonas reinhardtii* that the photoconversion efficiency was highest with a light intensity of $25\,\mu mol\,s^{-1}\,m^{-2}$ using 90% red and 10% blue LEDs.

Choice of medium and pH stability

Both OECD test guideline 201 (Organisation for Economic Co-operation and Development 2006) and ISO method 8692 (International Organization for Standardization 2012) proposed media with pH 8.1, but the stability of pH during exposure with complex samples can only be ensured by increasing the buffer capacity of these media.

The stability of pH was achieved by 10 mM 3-(N-morpholino) propanesulfonic acid buffer in the Talaquil medium (Le Faucheur et al. 2005). The pH was pH 7.7 in the Talaquil medium and in an experiment with diuron, the final pH after 24 h of exposure ranged between pH 7.77 and 8.01 with pH 7.94 in the control wells with algae. The *R. subcapitata* had a diameter of $4.4 \pm 0.2\,\mu m$ (5% CV, $n = 17$) at the beginning of exposure and a diameter of $4.1 \pm 0.1\,\mu m$ (2% CV, $n = 17$) after 24 h of exposure on the black clear-bottom plates.

In 2010, after the introduction of the combined algae test, a pH-stabilized modification of the ISO method 8692 medium (Altenburger et al. 2010) was developed that used 2 mM phosphate to buffer the pH together with 0.6 mM $NaHCO_3$, which kept the pH at 6.9 to 7.0 (Altenburger et al. 2010). On the 96-well plate, the pH in the Altenburger medium was stable, resulting in pH 7.28 ± 0.1 ($n = 3$) after 24-h growth on the well-plate. The cell size of *R. subcapitata* was slightly smaller, with a diameter of $3.7 \pm 0.1\,\mu m$ ($n = 3$), and the unexposed cells had a lower doubling time of 29 ± 9 h ($n = 3$).

As the cell size distributions shown in the Supplemental Data, Figure S9A demonstrate, *R. subcapitata* had a broader distribution with a sharper peak at 3-µm diameter in Altenburger medium, whereas the size distribution in Talaquil medium was more bell-shaped with a maximum approximate 4-µm diameter. The *R. subcapitata* tested in the present study were smaller than *C. reinhardtii* with red/blue LED illumination (Wagner et al. 2016). Wagner et al. (2016) had demonstrated for *C. reinhardtii* that size depended on the color of illumination. The *C. reinhardtii* were smaller when grown under red and blue LEDs than under warm-white light (Wagner 2016).

When exposed to varying concentrations of diuron, both populations shifted to smaller cell sizes, which was less pronounced for Talaquil medium (Supplemental Data, Figure S9B) than for Altenburger medium (Supplemental Data, Figure S9C). The following experiments were performed with Talaquil medium because some of the chemicals tested are ionogenic, and the complex mixtures also typically need a higher buffer capacity (Escher et al. 2020a).

Concentration–response curves curves and modeling

Diuron served as positive control for all endpoints of the combined algae test. The concentration–response curves of diuron were very similar between algae grown in Talaquil medium and Altenburger medium (Supplemental Data, Figure S10), with robust and well-repeatable effects for 2-h IPAM and 24-h IPAM and with only slightly lower sensitivity in Altenburger medium than in Talaquil medium for the growth rate endpoint. Cell counts are a more direct measure to derive growth rates. We used the CASY counter to quantify the cell number, which cannot be directly measured in the plates but had to be done manually after combining the volume of 2 wells that contained the same concentrations of diuron or unexposed cells. The $EC10_{cell\ count}$ was also derived from a 10-point serial dilution. In the Altenburger medium the $EC10_{growth\ rate}$ of $0.23 \pm 0.03\,\mu M$ from fluorescence measurements was indistinguishable from the $EC10_{cell\ count}$ of $0.24 \pm 0.03\,\mu M$ (Supplemental Data, Figure S10A). In the Talaquil medium the $EC10_{growth\ rate}$ of $0.10 \pm 0.02\,\mu M$ from fluorescence measurements was also close to the $EC10_{cell\ count}$ of $0.12 \pm 0.01\,\mu M$ for diuron (Supplemental Data, Figure S10B). The $EC10_{cell\ count}$ determined in Talaquil medium was more sensitive by a factor of 2 than in Altenburger medium.

Overall, the diuron EC10 showed good consistency over time (Supplemental Data, Figure S11). The measurement of the quantum yield of photosynthesis Y showed much less blur in the black clear-bottom plates than in the clear plates (Supplemental Data, Figure S12).

In both media, the growth endpoint measured via fluorescence showed a great deal of variability and sometimes an increasing growth rate at low doses, leading to apparent negative inhibition of growth. This was more or less severe

depending on the experiment and not systematic (see case study in the later section, *Algal toxicity of water samples* and Supplemental Data, Figure S21). Measurement of the inhibition of growth measured via optical density was often preferable for complex samples such as wastewater treatment plant influent and effluent (Supplemental Data, Figure S13). In work with nanoparticles, flow cytometric cell counts were applied for the combined algae test (Neale et al. 2015), which would be another more precise alternative to fluorescence measurements.

The wastewater treatment plant sample decreased the pH in both media to <pH 5, so the pH was adjusted to pH 7 in the medium before dosing the algae. All 3 wastewater samples showed a pattern distinctly different from diuron, with 24-h IPAM as most sensitive endpoint, followed by 24-h growth inhibition. No difference between the 2 media was observed (Supplemental Data, Figure S13).

Traditionally, log–logistic or related log–sigmoidal models were fitted to the concentration–response curves (Scholze et al. 2001). More recently, it has been demonstrated that at low effect levels (<30%), concentration–response curves become linear with nonlogarithmic concentrations (Escher et al. 2018a). This was especially advantageous for environmental samples of low contamination levels where large amounts of samples would have to be enriched to achieve sufficiently high effects to derive full concentration–response curves. These linear concentration–response curves were also introduced into the combined algae test, and low effect-level linear concentration–response curves (Equations 11 and 12) were compared with log–logistic concentration–response curves (Equations 9 and 10). As Supplemental Data, Figure S14 demonstrates for the individual PSII herbicides and other chemicals (see the later section, *Fingerprinting of individual PSII herbicides and other chemicals* for more details), there was an excellent agreement of EC10 values for the endpoint 2-h IPAM and 24-h IPAM and, apart from a few outliers, also for the 24-h growth rate.

We also compared the $EC10_{24h\ growth}$ from growth assessed via biomass and OD685 with the growth rate from F440/685 (Supplemental Data, Figure S15). There was a good agreement for more potent chemicals, with some more scatters for low-potency chemicals. In the following, we report only the EC10 from the linear concentration–response curves and the $EC10_{24h\ growth}$ using the growth rate from F440/685. However, we advise that for more difficult and highly contaminated samples than the wastewater treatment plant influent and effluent (Supplemental Data, Figure S13), the full log–logistic model with derivation of EC50 is preferable.

Baseline toxicity QSARs

The 7 baseline toxicants yielded concentration–response curves (Supplemental Data, Figure S16) that were consistent with those of previous studies (Escher et al. 2008; Tang and Escher 2014). For comparison, we derived the EC50 from log–logistic concentration–response curves, and the QSARs based on log (1/EC50) and the liposome/water partition constants log K_{lipw} (Vaes et al. 1997) agreed well with previous studies (Supplemental Data, Figure S17A), with slightly lower sensitivity of the EC50 in the present study.

Because EC10 values from low-level linear concentration–response curves were applied in the present study for surface water samples, we also developed QSARs based on log EC10 (Supplemental Data, Table S1 and Figure S17B). According to Equations 20 to 22, the confidence intervals of the QSARs for the 3 endpoints overlapped, with very similar slopes, and there was just a slight variation in the intercept of the QSAR equation.

$$\log(1/EC10_{2h\ IPAM}(M)) = (0.79 \pm 0.08) \times \log K_{lipw} + (1.17 \pm 0.26) \quad (20)$$
$$R^2 = 0.952, \quad n = 7, \quad F = 99.8$$

$$\log(1/EC10_{24h\ IPAM}(M)) = (0.71 \pm 0.14) \times \log K_{lipw} + (1.34 \pm 0.44) \quad (21)$$
$$R^2 = 0.846, \quad n = 7, \quad F = 27.4$$

$$\log(1/EC10_{24h\ growth\ rate}(M) = (0.75 \pm 0.08) \times \log K_{lipw} + (1.50 \pm 0.25) \quad (22)$$
$$R^2 = 0.940, \quad n = 6, \quad F = 62.2$$

These baseline QSARs were compared with previous baseline toxicity QSARs established for the combined algae test (Escher et al. 2008; Tang and Escher 2014) using EC50 values with excellent repeatability of the new set-up and illumination conditions. Furthermore, the similarity between the QSARs of the 3 different endpoints is consistent with the expectation of constant critical membrane burdens for baseline toxicity (McCarty and Mackay 1993).

Fingerprinting of individual PSII herbicides and other chemicals

All concentration–response curves of the individual chemicals (Supplemental Data, Table S2) are given in the Supplemental Data, Section S8 and Figure S18, and all EC10 and EC50 values are listed in the Supplemental Data, Table S3. The newly measured EC50s were in excellent agreement with previous studies (Tang and Escher 2014; Kienle et al. 2019; Figure S19). For all PSII inhibitors, $EC10_{2h\ IPAM}$ and $EC10_{24h\ IPAM}$ were very similar, but the $EC10_{24h\ growth}$ was 10.8 ± 5.6 times higher than the $EC10_{24h\ IPAM}$ (Supplemental Data, Table S3). This ratio $EC10_{24h\ growth}/EC10_{24h\ IPAM}$ was only 1.2 ± 1.2 for the baseline toxicants (Supplemental Data, Table S3).

It is possible to use the ratio $EC10_{24h\ growth}/EC10_{24h\ IPAM}$ as an indicator for mode-of-action classification with >5 likely to act as PSII inhibitor and <5 likely to act as baseline toxicant. A more precise indicator is the toxic ratio, which is the ratio between the EC10 predicted for baseline toxicity divided by the experimental EC10 (Maeder et al. 2004). If the toxic ratio is >10, a chemical is classified as specifically acting. In case of the endpoint 2-h IPAM a toxic ratio >10 means that the mode of action is PSII inhibition.

For growth, any excess toxic ratio could also be caused by a different specific mode of action, but this did not apply to any of the chemicals in the test set. Apart from benzothiazole-2-sulfonic acid, whose log D_{lipw} was only predicted and hence uncertain, all chemicals that were not PSII herbicides or their transformation products were confirmed as baseline toxicants with toxic ratio <10 for all endpoints (Supplemental Data, Table S3).

The specificity of PSII herbicides was very high, with toxic ratio$_{2h\ IPAM}$ ranging from 2×10^6 for bromacil down to 340 for bentazone. For the PSII herbicides toxic ratio$_{24h\ IPAM}$ was typically in the same range as toxic ratio$_{2h\ IPAM}$, but the toxic ratio$_{24h\ growth}$ was typically approximately 20 times lower. In contrast, for the baseline toxicants (or chemicals with other modes of action that acted as baseline toxicants in the combined algae test), the EC10 did not differ much between the 3 endpoints, and the toxic ratios remained <10 (Supplemental Data, Table S3).

The transformation products of PSII herbicides were typically less hydrophobic and less potent than their parent compounds. Atrazine-desethyl and atrazine-desisopropyl had a toxic ratio reduced by factors of 9 and 18, respectively, compared with atrazine (toxic ratio ~60′000 for PSII inhibition), but their toxic ratios were still >1000, indicating specific herbicidal activity (Figure 2A). Atrazine-2-hydroxy lost its herbicidal potency; no EC10 could be derived for 2-h IPAM and 24-h IPAM, and the toxic ratio$_{24h\ growth}$ was only 28 (Figure 2A).

Terbuthylazine and its transformation products showed a similar picture: terbuthylazine-desethyl had almost as high a toxic ratio as the parent terbuthylazine but is less hydrophobic (Figure 2B). Terbuthylazine-2-hydroxy was less potent but still had a toxic ratio >1000 for the PSII inhibition endpoints (Figure 2B). Terbuthylazine-desethyl-2-hydroxy lost its specificity entirely and was not active up to the highest tested concentration of 2×10^{-4} M, so it is clearly only baseline toxic. Diuron-desdimethyl (3,4-dichlorophenylurea) also lost only a little of its parent diuron's hydrophobicity, but it lost its specificity, with the toxic ratio decreasing from 71 000 for diuron to 130 for diuron-desdimethyl in 2-h IPAM (Supplemental Data, Table S3). This is consistent with previous work on the combined algae test in which the toxic ratio decreased from 89 000 to 137 for 2-h IPAM (Neuwoehner et al. 2010).

One can also note that the solvent DMSO acted as baseline toxicant (toxic ratio = 2) for growth rate inhibition with an EC10$_{24h\ growth\ rate}$ of 0.13 ± 0.01 M (0.8 ± 0.1%; V_{DMSO}:V_{medium}). No inhibition of photosynthesis was observed for DMSO. In all experiments, the DMSO content was kept at <0.5%. Methanol used as solvent in the water extracts was typically evaporated prior to addition of the medium. Directly tested, the EC10$_{2h\ IPAM}$ of methanol was 0.89 ± 0.04 M (3.6%; $V_{methanol}$:V_{medium}) and the EC10$_{24h\ IPAM}$ was 0.18 ± 0.01 M (0.7%), with no effect on growth rate. The toxic ratios were 0.02 and 0.07 respectively, indicating that methanol acted as baseline toxicant with the caveat that a substantial fraction of methanol had most likely evaporated during the exposure.

Algal toxicity of water samples

We tested water samples from a small river (Supplemental Data, Figure S20) that had previously been characterized with a panel of in vitro bioassays (Müller et al. 2018). All concentration–response curves are depicted in the Supplemental Data, Figure S21, and the EC10 values are listed in the Supplemental Data, Table S4. Prior to the introduction of the wastewater treatment plant effluent, the river water R1 to R3 had low effects; 24-h IPAM and 24-h growth inhibition was even below the limit of detection (Figure 3). The effluent had much lower EC10 values, and these higher effects were diluted in the river water (R4) and attenuated downstream of the wastewater treatment

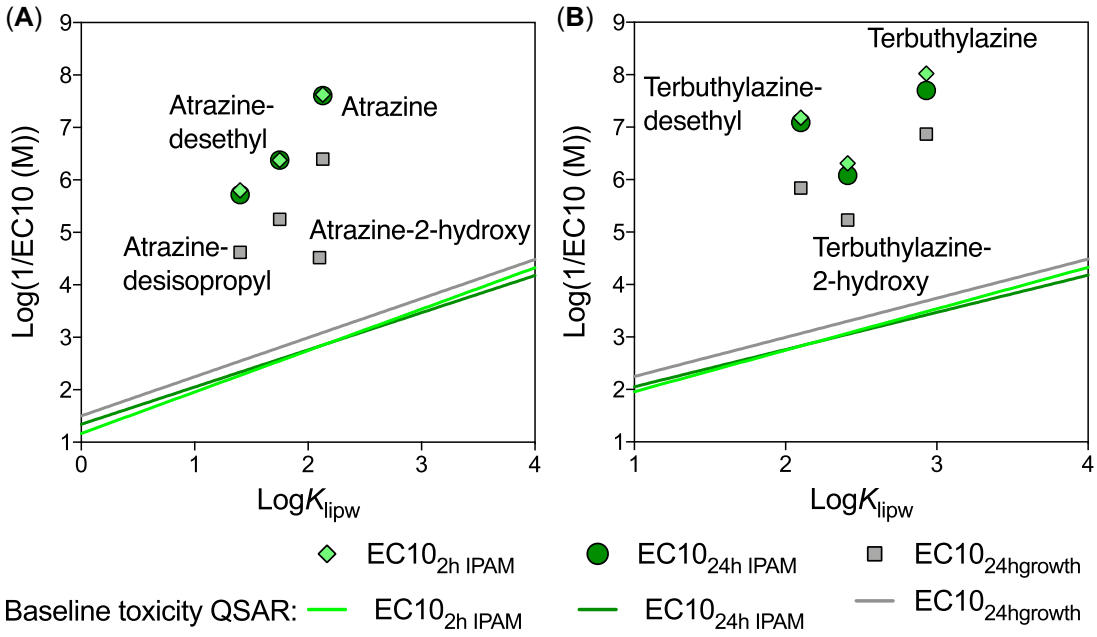

FIGURE 2: Toxic ratio analysis of (**A**) atrazine and its transformation products, and (**B**) terbuthylazine and its transformation products. The lines correspond to the baseline toxicity quantitative structure–activity relationships (QSARs; Equations 20–22). EC10 = effect concentration, 10%.

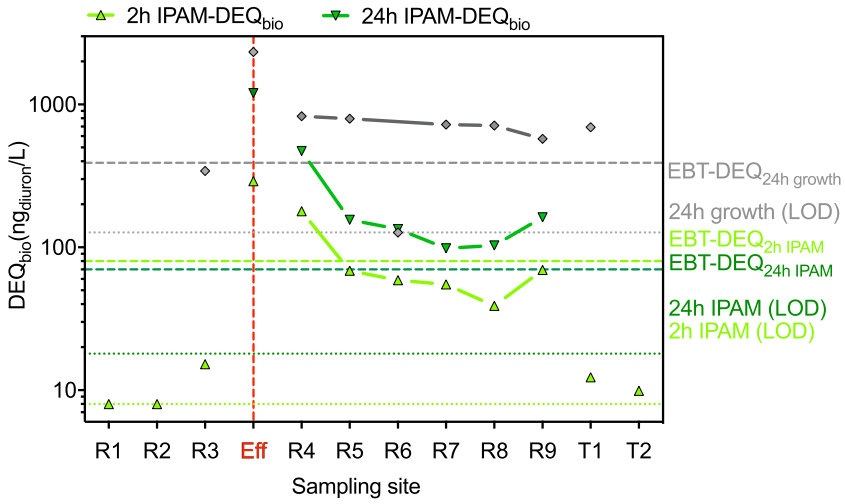

FIGURE 3: Algal toxicity at the sampling sites along a river (R1–R9) with wastewater treatment plant effluent (Eff) introduced between R3 and R4, in comparison with the tributaries T1 and T2. The map of the sampling sites is in Supplemental Data, Figure S20. IPAM-DEQ = Maxi-Imaging pulse-amplitude modulated-diuron equivalent concentration; EBT = effect-based trigger values; LOD = limit of detection.

plant (R5–R9; Figure 3). Above the wastewater treatment plant at R2 and R3, the 2-h IPAM was the most sensitive endpoint (Figure 3), indicating that algal toxicity stemmed from PSII herbicides. This changed with the introduction of wastewater treatment plant effluent, when the 24-hIPAM became more sensitive, presumably owing to a large contribution of non-herbicidal chemicals. This pattern ($EC10_{24h\ IPAM} < EC10_{2h\ IPAM}$) continued down the main river stem (R4–R9). For the tributaries T1 and T2, there were very low effects, mostly below detection limits (Figure 3), but now only 2-h IPAM was detectable, indicating that the small load of effects stemming from the tributaries was due to PSII herbicides.

Effect-based trigger values for algal toxicity

We had previously derived effect-based trigger values (EBTs) for the 2-h IPAM endpoint for different water types by reading across from different Australian guidelines (Tang and Escher 2014). In this derivation we used the lower fifth percentile of a distribution of all DEQs corresponding to the guideline values. The resulting $EBT\text{-}DEQ_{2h\ IPAM}$ values were 0.54 μg_{diuron}/L for surface water, 0.63 μg_{diuron}/L for recycled water for indirect potable reuse, and 0.44 μg_{diuron}/L for drinking water.

In 2018, we also read across from the European Union's Water Framework Directive Environmental Quality Standards (EQS; European Commission 2010) using Equation 23 (Escher et al. 2018b). In the present study, we did not use a low percentile of the distribution of all DEQ_i but the mean of all DEQ_i for chemicals i with $EC50_i/EQS_i < 1000$ (i.e., only for chemicals for which the herbicidal activity had been included in derivation of the EQS).

$$EBT = \frac{\sum_{i=1}^{n} DEQ_i}{n} = \frac{1}{n}\sum_{i=1}^{n} C_i \times REP_i \qquad (23)$$

For European surface water the $EBT\text{-}DEQ_{2h\ IPAM}$ was 0.07 μg_{diuron}/L, and the $EBT\text{-}DEQ_{24h\ growth}$ was 0.13 μg_{diuron}/L (Escher 2018b). These values were derived from 12 EC50s for single chemicals.

With the new collection of experimental data on EC10s from linear concentration–response curves in the Supplemental Data, Table S3, we revised the EBT-DEQ using the template given in Escher et al. (2018b). We now had overall data for 17 chemicals available; only 11 of them fulfilled the criteria for inclusion because the rest were baseline toxic, and the $EBT\text{-}DEQ_{2h\ IPAM}$ was 0.08 μg_{diuron}/L, the $EBT\text{-}DEQ_{24h\ IPAM}$ was 0.07 μg_{diuron}/L, and the $EBT\text{-}DEQ_{24h\ growth}$ was 0.39 μg_{diuron}/L. The similarity to previously derived EBTs demonstrates the robustness of the experimental data and the approach to deriving EBTs.

All DEQ_{bio} values were below the EBT-DEQ upstream of the wastewater treatment plant (Figure 3). The effluent exceeded the EBT-DEQ for all endpoints. The first site at the river (R4) was heavily impacted by the effluent, and then the effect decreased downstream in a similar fashion to chemicals and their cytotoxicity and effect in other in vitro assays (Müller et al. 2018). The 2-h $IPAM\text{-}DEQ_{bio}$ fell below the $EBT\text{-}DEQ_{2h\ IPAM}$ downstream of site R4, and the tributaries were also of good quality with respect to algal toxicity. The 24-h IPAM and growth endpoints marginally exceeded the associated $EBT\text{-}DEQ_{24h\ IPAM}$ and $EBT\text{-}DEQ_{24h\ growth}$, presumably because nonherbicides had contributed to the mixture effects. This hypothesis was further explored by iceberg modeling.

Iceberg modeling: Comparison of chemical analysis and bioassay results

In all, 329 chemicals were detected in one or more of the water samples, and 204 of them were below the detection limit. All concentrations are listed in the Supplemental Data, Table S5, and a heat map is depicted in the Supplemental Data, Figure S22 for all chemicals and in Figure S23 for the chemicals with effect data. Effect data were available for 25 detected PSII herbicides and their degradation products and for 13 other chemicals.

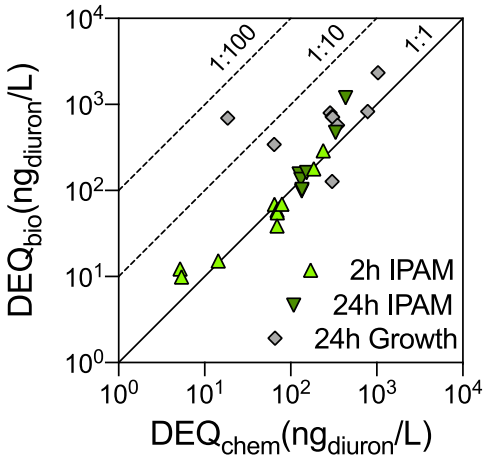

FIGURE 4: Comparison of diuron equivalent concentrations (DEQ_{bio}; Equation 14) and DEQ_{chem} (Equation 16) for all 3 endpoints of the combined algae test: 2-h IPAM-DEQ and 24-h IPAM-DEQ for inhibition of photosynthesis and 24-h growth DEQ for inhibition of growth rate. IPAM-DEQ = Maxi-Imaging pulse-amplitude modulated-diuron equivalent concentration.

Diuron did not exceed the annual average EQS of 0.2 µg/L (European Commission 2010), nor did it exceed the Swiss EQS of 0.07 µg/L (Schweizerischer Bundesrat 2020). Terbutryn exceeded the EQS of 0.065 µg/L set in Switzerland (Schweizerischer Bundesrat 2020) only at R4. The legacy PSII herbicide atrazine, which was phased out in Germany beginning in 1991, could still be detected at a level of 100 times lower than the EQS, and its concentrations were higher upstream of the wastewater treatment plant than downstream.

The detected chemicals and their 2-h IPAM-DEQ_{chem} and 24-h IPAM-DEQ_{chem} explained the measured inhibition of photosynthesis 2-h IPAM-DEQ_{chem} and 24-h IPAM-DEQ_{bio} quite well, despite 2 outliers for 24-h growth-DEQ_{bio} (Figure 4).

The concentrations were dominated by the nonherbicides (other chemicals), with concentrations in the range of 1 to 140 µg/L for 1H-benzotriazole and N-acetyl- and N-formyl-4 aminoantiyprine, whereas the PSII herbicides were present at levels of 100 ng/L and less (Figure 5A). When the concentrations were translated to 2-h IPAM-DEQ_{chem}, 1H-benzotriazole and triclosan had a very moderate contribution to 2-h IPAM-DEQ_{chem}, but 2-h IPAM-DEQ_{chem} was dominated by potent PSII inhibitors (Figure 5B). Dominant by far was terbutryn, which is equipotent to diuron (Supplemental Data, Table S3), but occurred at much higher concentrations (Supplemental Data, Table S5). Diuron, isoproturon, and atrazine also contributed substantially to 2-h IPAM-DEQ_{chem}. Of the degradation products of PSII herbicides, atrazine-desethyl, terbuthylazine-2-hydroxy, and terbuthylazine-desethyl contributed to 2-h IPAM-DEQ_{chem}, but others had either low potency or low abundance. None of the other PSII herbicides exceeded the EQS.

The PSII herbicides explained most of the DEQ_{chem} for the 2-h IPAM (Figure 5) and 24-h IPAM, with other chemicals contributing <0.2%. The 15 PSII herbicides explained 101% (minimum 43%, maximum 178%, and 95% confidence interval [CI] 74–128%) of the 2-h IPAM-DEQ_{bio}, and 92% (minimum 36%, maximum 136%, and 95% CI 60–124%) of the 24-h IPAM-DEQ_{bio}. Only for 24-h growth-DEQ_{bio} did the other chemicals play a more important role, with diclofenac and triclosan contributing up to 2% to 24-h growth-DEQ_{bio}. The contribution of other chemicals to growth inhibition is also evidenced by the fact that overall a smaller fraction of effect could be explained by the 38 chemicals with effect data (Figure 5), with 43% (minimum 3%, maximum 95%,

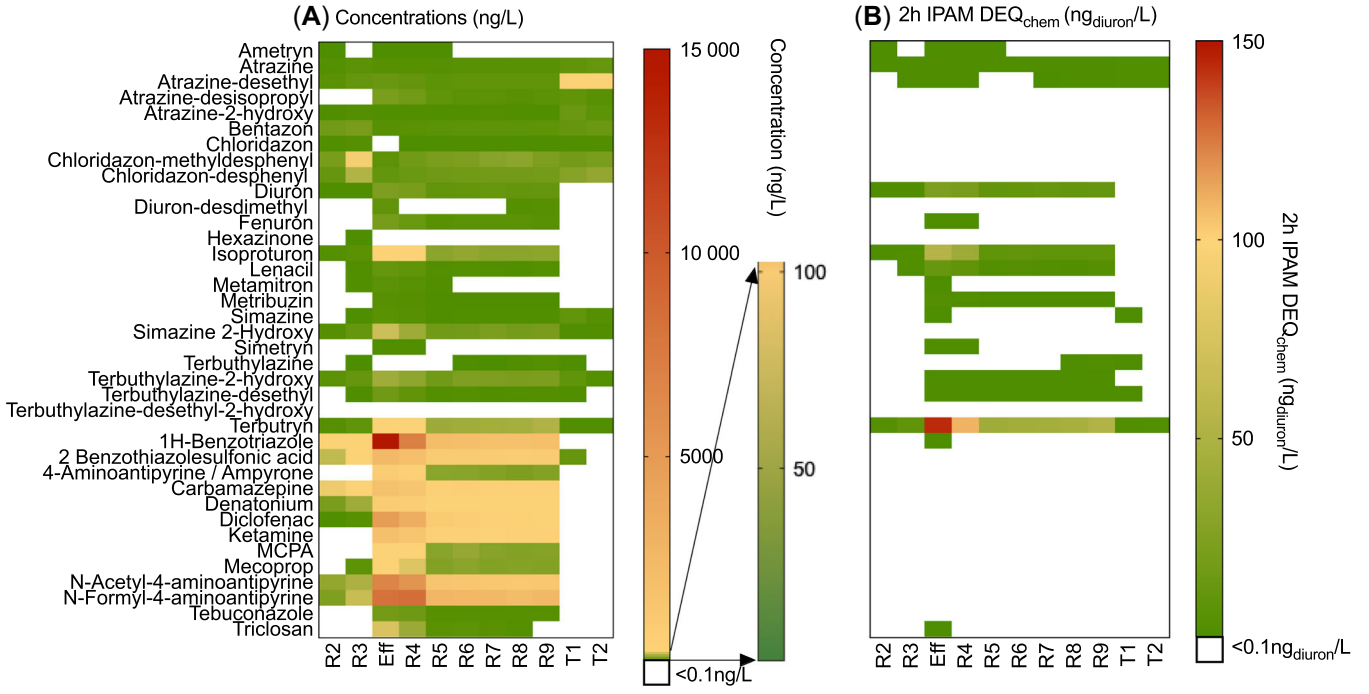

FIGURE 5: (**A**) Concentrations and (**B**) 2-h IPAM-DEQ_{chem} of the 38 chemicals for which algal toxicity data were available in the water samples. (For sample code see Supplemental Data, Table S4.) IPAM-DEQ = Maxi-Imaging pulse-amplitude modulated-diuron equivalent concentration.

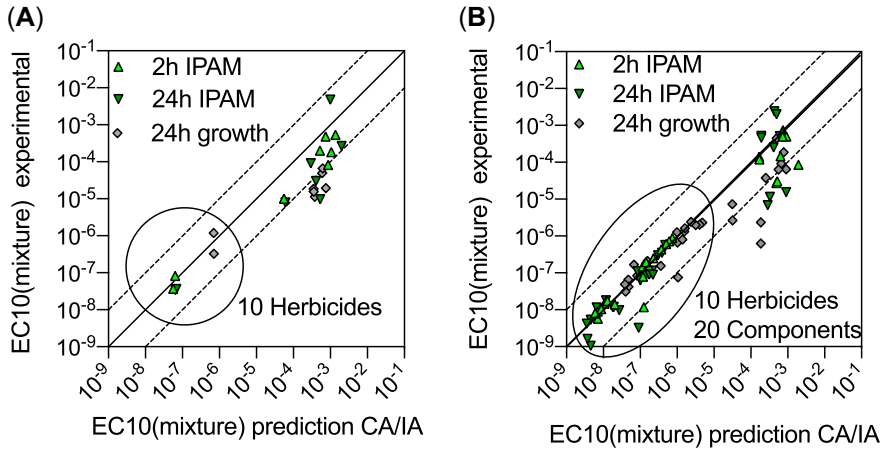

FIGURE 6: Comparison of predicted (CA) and experimental mixture effects for the different combinations of (**A**) equipotent mixtures of 10 photosystem II (PSII) herbicides, 10 other chemicals, and all 20 chemicals, and (**B**) mixtures of chemicals in concentration ratios as they occurred in the water samples. Encircled are the mixtures with 10 PSII herbicides and 20 chemicals. IPAM-DEQ = Maxi-Imaging pulse-amplitude modulated; EC10 = effect concentration, 10%; CA = concentration addition; IA = and independent action.

and 95% CI 20–66%) of 24-h growth-DEQ_{bio}. That PSII herbicides dominate the mixture effects in algae of wastewater samples has already been previously demonstrated (Tang and Escher 2014; Kienle et al. 2019). In a surface water quality assessment study in The Netherlands (de Baat et al. 2018), the PSII herbicides desethylterbuthylazine, dimethenamid, and linuron exceeded water quality standards, but the first 2 did not contribute to photosynthesis inhibition. Linuron could explain the detected algal toxicity (de Baat et al. 2018).

Designed mixture experiments

Mixture experiments were performed with 10 of the most relevant PSII herbicides and 10 nonherbicidal chemicals that had been detected in the river water and effluent samples. The concentration–response curves are depicted in the Supplemental Data, Figure S24, and the EC10 values derived from them are listed in the Supplemental Data, Table S6. When the 10 PSII herbicides were mixed in the concentration ratios of their EC10s of the endpoints 2-h IPAM and 24-h IPAM, the resulting mixture effects were very close to the prediction by the concentration addition/independent action model for the 3 experimentally determined endpoints (encircled in Figure 6 and detailed in the Supplemental Data, Figure S25A). In contrast, the mixtures of the 10 other chemicals and of all 20 chemicals proved to be much more potent than predicted from concentration addition and the EC10 of the single compounds. In particular, the EC10 for growth inhibition was more than a factor of 10 lower than predicted by the concentration addition/independent action model (Figure 6A and detailed in the Supplemental Data, Figure S25B and C). Mansano et al. (2017) also reported synergistic interactions between diuron and carbofuran, whose potencies differ by more than 1000-fold, making the mixture experiments difficult to perform. Given the relatively high uncertainty of the effect concentrations of the low-potency nonherbicides, this does not mean that synergy can be invoked but rather reflects the difficulty of quantifying effects for nonherbicides.

The same 10 PSII herbicides, 10 other chemicals, and all 20 together were mixed in the same concentration ratios as were detected in the water samples (Supplemental Data, Table S5), and the resulting concentration–response curves are depicted in the Supplemental Data, Figure S26. Whenever PSII herbicides were included in the mixtures, there was an excellent agreement between the experiment and the prediction by the concentration addition/independent action model (Figure 6B), whereas the mixtures of 10 nonherbicides did not show such a good agreement with the measured mixture effects, which were often higher than predicted by the joint concentration addition/independent action model, pointing to the same uncertainty as for the equipotent mixtures.

CONCLUSIONS

The combined algae test has been improved substantially since its initial development in 2008. In particular, the dichromatic red/blue LED illumination helped boost growth rate in black clear-bottom 96-well plates. The illumination box was a prototype custom-built in our workshop, and the homogeneity of the illumination was acceptable but has further potential for improvement.

The use of black clear-bottom plates greatly improved the precision of the IPAM measurements but also allowed fluorescence measurements to deduce the growth rate. Despite the higher growth rates, the endpoint inhibition of growth rate did not meet our quality expectations, presumably due to interference by autofluorescence of the samples despite modifications of the equations to account for this. Better results were obtained for wastewater treatment plant samples using optical density to quantify biomass inhibition. An alternative proxy for cell count could be flow cytometry measurement. Such an instrument was not available in the present study but

has previously been proved compatible with Maxi-Imaging PAM measurements in a modification of the combined algae test (Neale et al. 2015).

Although the combined algae test is slightly less sensitive than the OECD test guideline 201 assay for the endpoint of growth inhibition (Organisation for Economic Co-operation and Development 2006), it has the advantage of the 2 additional endpoints of photosynthesis inhibition after 2 and 24 h, which are much more sensitive to the PSII inhibitors that typically dominate the mixture toxicity in algae. Furthermore, thanks to the set-up on a 96-well plate, the combined algae test is much simpler to perform routinely, especially when aided by a pipetting robot, and it allows a much higher throughput of chemicals and samples than any other algae assays. A compromise had to be struck when it came to cell numbers because the growth inhibition assay according to OECD test guideline 201 (Organisation for Economic Co-operation and Development 2006) requests much lower cell densities than is possible for concomitant Maxi-Imaging PAM measurements. Shortening the incubation time to 24 h also helps with increasing sample throughput and is less critical with respect to growth in 96-well plates that cannot be shaken effectively, so eventually CO_2 would become limiting, even if additional buffer were supplemented. Evaporation would also become more of an issue if the exposure duration were further extended.

In its present form the combined algae test is suitable for monitoring surface water quality, and the interpretation of detected effects can be greatly enhanced with the revised effect-based trigger values and the iceberg modeling.

Supplemental Data—The Supplemental Data are available on the Wiley Online Library at https://doi.org/10.1002/etc.4873.

Acknowledgment—We thank the Swiss Centre for Applied Ecotoxicology for continued support of the combined algae test and are grateful to N. Bramaz, C. Kienle, M. Junghans, A. Schifferli, and E. Vermeirssen for their input over many years. R. Schlichting coordinated the experimental work and instruments and we thank her, L. Henneburger, J. Huchthausen, C. Kienle, L. Niu, N. Sossalla, and C. Zarfl for review of the manuscript. We thank R. Altenburger, S. Aulhorn, and M. Schmitt-Jansen for helpful discussions. We thank J. Knittel, who designed the illumination set up, and the Helmholtz Center for Environmental Research workshop for building prototypes and the final light box. Particular thanks go to A. Naumann, R. Angeli, N. Hoffmann, P. Portius, and S. Wagner. We thank M.E. Müller and C. Zwiener for provision of surface water sample extracts and M. Schwientek for the map of the sampling sites. We are grateful to M. Krauss for LC/MS analysis of the surface water samples. N. Sossalla provided the samples of wastewater treatment plant influent and effluent. S. Schöne proofread the manuscript. The present study was supported by the Collaborative Research Centre 1253 CAMPOS (Project P1: Rivers), funded by the German Research Foundation (DFG; grant SFB 1253/1 20147). The algae assays were performed using equipment of the robotic platform CITEPro (Chemicals in the Environment Profiler) funded by the Helmholtz Association. Open access funding enabled and organized by Projekt DEAL.

Disclaimer—All authors have no interest to declare. The views expressed in the present review are solely those of the authors.

Author Contribution Statement—B. Escher developed the study concept, evaluated the data, and wrote the paper. L. Glauch optimized and performed all experiments.

Data Availability Statement—Data, associated metadata, and calculation tools are available from the corresponding author (beate.escher@ufz.de).

REFERENCES

Altenburger R, Krueger J, Eisentraeger A. 2010. Proposing a pH stabilised nutrient medium for algal growth bioassays. *Chemosphere* 78:864–870.

de Baat ML, Bas DA, van Beusekom SAM, Droge STJ, van der Meer F, de Vries M, Verdonschot PFM, Kraak MHS. 2018. Nationwide screening of surface water toxicity to algae. *Sci Total Environ* 645:780–787.

Di Paolo C, Ottermanns R, Keiter S, Ait-Aissa S, Bluhm K, Brack W, Breitholtz M, Buchinger S, Carere M, Chalon C, Cousin X, Dulio V, Escher BI, Hamers T, Hilscherova K, Jarque S, Jonas A, Maillot-Marechal E, Marneffe Y, Nguyen MT, Pandard P, Schifferli A, Schulze T, Seidensticker S, Seiler TB, Tang J, van der Oost R, Vermeirssen E, Zounkova R, Zwart N, Hollert H. 2016. Bioassay battery interlaboratory investigation of emerging contaminants in spiked water extracts—Towards the implementation of bioanalytical monitoring tools in water quality assessment and monitoring. *Water Res* 104:473–484.

Eisentraeger A, Brinkmann C, Michel K, Hahn S, Huettner M, Weber G. 2004. Development of automated high-throughput ecotoxicity and genotoxicity test systems and fields of application. *Water Sci Technol* 50:109–114.

Eisentraeger A, Dott W, Klein J, Hahn S. 2003. Comparative studies on algal toxicity testing using fluorometric microplate and Erlenmeyer flask growth-inhibition assays. *Ecotoxicol Environ Saf* 54:346–354.

Escher BI, Abagyan R, Embry M, Klüver N, Redman AD, Zarfl C, Parkerton TF. 2020a. Recommendations for improving methods and models for aquatic hazard assessment of ionizable organic chemicals. *Environ Toxicol Chem* 39:269–286.

Escher BI, Ait-Aissa S, Behnisch PA, Brack W, Brion F, Brouwer A, Buchinger S, Crawford S, Hamers THM, Hettwer K, Hilscherova K, Hollert H, Kase R, Kienle C, Legradi J, Tuerk J, van der Oost R, Vermeirssen E, Neale PA. 2018b. Effect-based trigger values for *in vitro* and *in vivo* bioassays performed on surface water extracts supporting the environmental quality standards (EQS) of the European Water Framework Directive. *Sci Total Environ* 628–629:748–765.

Escher BI, Bramaz N, Mueller JF, Quayle P, Rutishauser S, Vermeirssen ELM. 2008. Toxic equivalent concentrations (TEQs) for baseline toxicity and specific modes of action as a tool to improve interpretation of ecotoxicity testing of environmental samples. *J Environ Monit* 10:612–621.

Escher BI, Bramaz N, Ort C. 2009. JEM Spotlight: Monitoring the treatment efficiency of a full scale ozonation on a sewage treatment plant with a mode-of-action based test battery. *J Environ Monit* 11:1836–1846.

Escher BI, Braun G, Zarfl C. 2020b. Exploring the concepts of concentration addition and independent action using a linear low-effect mixture model. *Environ Toxicol Chem*. https://doi.org/10/1002/etc.4868

Escher BI, Glauch L, Konig M, Mayer P, Schlichting R. 2019. Baseline toxicity and volatility cutoff in reporter gene assays used for high-throughput screening. *Chem Res Toxicol* 32:1646–1655.

Escher BI, Neale PA, Villeneuve D. 2018a. The advantages of linear concentration-response curves for *in vitro* bioassays with environmental samples. *Environ Toxicol Chem* 37:2273–2280.

European Commission. 2010. Common Implementation Strategy for the Water Framework Directive (2000/60/EC). Technical Guidance for Deriving Environmental Quality Standards. WG E(9)–10-03e–TGD-EQS. Brussels, Belgium.

Fai PB, Grant A, Reid B. 2007. Chlorophyll a fluorescence as a biomarker for rapid toxicity assessment. *Environ Toxicol Chem* 26:1520–1531.

International Organization for Standardization. 2012. ISO 8692: Water quality—Freshwater algal growth inhibition test with unicellular green algae, update from ISO 8692:2004. Geneva, Switzerland.

Kienle C, Vermeirssen ELM, Schifferli A, Singer H, Stamm C, Werner I. 2019. Effects of treated wastewater on the ecotoxicity of small streams—Unravelling the contribution of chemicals causing effects. *PLoS One* 14:0226278.

Le Faucheur S, Behra R, Sigg L. 2005. Phytochelatin induction, cadmium accumulation, and algal sensitivity to free cadmium ion in *Scenedesmus vacuolatus*. *Environ Toxicol Chem* 24:1731–1737.

Maeder V, Escher BI, Scheringer M, Hungerbuhler K. 2004. Toxic ratio as an indicator of the intrinsic toxicity in the assessment of persistent, bioaccumulative, and toxic chemicals. *Environ Sci Technol* 38:3659–3666.

Mansano AS, Moreira RA, Dornfeld HC, Freitas EC, Vieira EM, Sarmento H, Rocha O, Seleghim MHR. 2017. Effects of diuron and carbofuran and their mixtures on the microalgae *Raphidocelis subcapitata*. *Ecotoxicol Environ Saf* 142:312–321.

Margot J, Kienle C, Magnet A, Weil M, Rossi L, de Alencastro LF, Abegglen C, Thonney D, Chevre N, Scharer M, Barry DA. 2013. Treatment of micropollutants in municipal wastewater: Ozone or powdered activated carbon? *Sci Total Environ* 461:480–498.

McCarty LS, Mackay D. 1993. Enhancing ecotoxicological modeling and assessment. *Environ Sci Technol* 27:1719–1728.

Mestankova H, Escher B, Schirmer K, von Gunten U, Canonica S. 2011. Evolution of algal toxicity during (photo)oxidative degradation of diuron. *Aquat Toxicol* 101:466–473.

Müller ME, Escher BI, Schwientek M, Werneburg M, Zarfl C, Zwiener C. 2018. Combining in vitro reporter gene bioassays with chemical analysis to assess changes in the water quality along the Ammer River, Southwestern Germany. *Environ Sci Eur* 30:20.

Neale PA, Braun G, Brack W, Carmona E, Gunold R, Konig M, Krauss M, Liebmann L, Liess M, Link M, Schafer RB, Schlichting R, Schreiner VC, Schulze T, Vormeier P, Weisner O, Escher BI. 2020. Assessing the mixture effects in in vitro bioassays of chemicals occurring in small agricultural streams during rain events. *Environ Sci Technol* 54:8280–8290.

Neale PA, Jaemting AK, O'Malley E, Herrmann J, Escher BI. 2015. Behaviour of titanium dioxide and zinc oxide nanoparticles in the presence of wastewater-derived organic matter and implications for algal toxicity. *Environ Sci Nano* 2:86–93.

Neale PA, Munz NA, Ait-Aissa S, Altenburger R, Brion F, Busch W, Escher BI, Hilscherova K, Kienle C, Novak J, Seiler T-B, Shao Y, Stamm C, Hollender J. 2017. Integrating chemical analysis and bioanalysis to evaluate the contribution of wastewater effluent on the micropollutant burden in small streams. *Sci Total Environ* 576:785–795.

Neuwoehner J, Zilberman T, Fenner K, Escher BI. 2010. QSAR analysis and mixture toxicity as diagnostic tools: Influence of degradation on the toxicity and mode of action of diuron in algae and daphnids. *Aquat Toxicol* 100:377.

Nivala J, Neale PA, Haasis T, Kahl S, König M, Müller R, Reemtsma T, Schlichting R, Escher B. 2018. Application of bioanalytical tools to evaluate treatment efficacy of conventional and intensified treatment wetlands. *Environ Sci Water Res Technol* 4:206–217.

Organisation for Economic Co-operation and Development. 2006. Guideline no. 201: Freshwater alga and cyanobacteria, growth inhibition test. Adopted: 23 March 2006. Annex 5 corrected: 28 July 2011. *OECD Guidelines for the Testing of Chemicals*. Paris, France.

Scholze M, Boedeker W, Faust M, Backhaus T, Altenburger R, Grimme LH. 2001. A general best-fit method for concentration-response curves and the estimation of low-effect concentrations. *Environ Toxicol Chem* 20:448–457.

Schreiber U, Quayle P, Schmidt S, Escher BI, Mueller JF. 2007. Methodology and evaluation of a highly sensitive algae toxicity test based on multiwell chlorophyll fluorescence imaging. *Biosens Bioelectron* 22:2554–2563.

Schweizerischer Bundesrat. 2020. Swiss ordinance 814.201. Gewässerschutzverordnung (GSchV). [cited 2020 September 9]. Available from: https://wwwadminch/opc/de/classified-compilation/19983281/indexhtml

Tang JYM, Escher BI. 2014. Realistic environmental mixtures of micropollutants in wastewater, recycled water and surface water: Herbicides dominate the mixture toxicity towards algae. *Environ Toxicol Chem* 33:1427–1436.

Tang JYM, Glenn E, Aryal R, Gernjak W, Escher BI. 2013. Toxicity characterization of urban stormwater with bioanalytical tools. *Water Res* 47:5594–5606.

Vaes WHJ, Ramos EU, Hamwijk C, vanHolsteijn I, Blaauboer BJ, Seinen W, Verhaar HJM, Hermens JLM. 1997. Solid phase microextraction as a tool to determine membrane/water partition coefficients and bioavailable concentrations in in vitro systems. *Chem Res Toxicol* 10:1067–1072.

Vaes WHJ, Ramos EU, Verhaar HJM, Hermens JLM. 1998. Acute toxicity of nonpolar versus polar narcosis: Is there a difference? *Environ Toxicol Chem* 17:1380–1384.

Vermeirssen ELM, Hollender J, Bramaz N, van der Voet J, Escher BI. 2010. Linking toxicity in algal and bacterial assays with chemical analysis in passive samplers deployed in 21 treated sewage effluents. *Environ Toxicol Chem* 29:2575–2582.

Vogs C, Kuehnert A, Hug C, Kuester E, Altenburger R. 2015. A toxicokinetic study of specifically acting and reactive organic chemicals for the prediction of internal effect concentrations in *Scenedesmus vacuolatus*. *Environ Toxicol Chem* 34:100–111.

Wagner I, Steinweg C, Posten C. 2016. Mono- and dichromatic LED illumination leads to enhanced growth and energy conversion for high-efficiency cultivation of microalgae for application in space. *Biotechnol J* 11:1060–1071.

